

## Simulations of Hydrodynamic Flows during Streamer Propagation in Dielectric Liquids

A. L. Kupershtokh and D. A. Medvedev

Lavrentyev Institute of Hydrodynamics RAS, Novosibirsk, 630090,  
RUSSIA

### Abstract

This paper presents the results of a computation of gas-dynamic flows accompanying different stages of the electric breakdown in dielectric liquids. The expansion of a rectilinear channel in the plane and cylindrical cases was considered under conditions leading to self-similar flow. The inner structure of the liquid-“plasma” transition layer was investigated. The computations were carried out of flows with shock waves that are generated during the propagation of the tip of a single streamer and during the growth of a branched streamer structure. Different regimes of the streamer growth in viscous dielectric liquids were considered.

### Introduction

Gas-dynamic flows play a decisive role in the process of streamer propagation in the electric breakdown in dielectric liquids. In the present paper we consider several stages of streamer development.

When energy releases in a thin uniform rectilinear conductive channel, the temperature and the pressure increase in it and the channel expands forming a divergent shock wave. The interface between the conductive channel and the surrounding liquid cannot be considered as an impenetrable piston but it represents a certain liquid-“plasma” transition layer in which the conversion of the liquid into a conductive phase of lower density takes place. This layer has a non-monotonic inner structure because of the influence of viscosity.

The propagation of the streamer tip results in formation of compression waves that propagate with the sound velocity in a dielectric liquid. When the tip velocity is supersonic, a divergent shock wave is formed.

Experiments show that the streamer growth generally begins from the tips of the existing structure (tip ramification). As this takes place, a complex pattern of interference of shock waves diverging from different tips arises.

### Lattice gas methods

The lattice gas (LG) method [1] treats a liquid flow as the dynamics of special particles which can move along the links of a fixed lattice and suffer collisions and scattering at the nodes. The LG method is in a sense an extremely simplified method of molecular dynamics. Another modification of this method is the method of immiscible lattice gases (ILG). Here two kinds (colors) of particles exist, one for a dielectric liquid and the second for a conductive phase. Collision

rules are chosen to maximize the flux of particles of given color to adjacent nodes with the majority of particles of the same color. This gives rise to surface tension at the interface.

### "Lattice Boltzmann Equation" (LBE) method

This method has evolved from the LG method. There are also particles that can move on a regular spatial lattice, and only a few velocity values are possible at each node. However, in contrast to the LG method, the local one-particle distribution functions  $N_i$  are taken as variables. Averaging completely eliminates statistical noise and allows one to reduce considerably the number of grid points in the computation domain. One should, however, give up integer arithmetic. The LBE method can be considered as a solution of the kinetic equation for a certain model system. The evolution equation is formally the same as for the LG

$$N_i(\vec{x} + \vec{c}_i, t + \Delta t) - N_i(\vec{x}, t) = \Omega_i(N(\vec{x} + \vec{c}_i, t + \Delta t)).$$

We used a collision operator in the BGK form [2], which means relaxation to the local equilibrium  $\Omega_i(N) = N_i - (N_i - N_i^{eq})/\tau$ . The equilibrium distribution functions  $N_i^{eq}$  depend on the local density  $\rho = \sum N_i$ , flow velocity  $\vec{u} = (\sum \vec{c}_i N_i)/\rho$ , and temperature, so that the conservation laws for mass, momentum, and energy are satisfied. In the BGK model, the relaxation time  $\tau$  governs the transport coefficients: viscosity, heat conductivity and diffusion coefficient ( $1/2 \leq \tau < \infty$ ). In our computations, we used a model with four velocity values 0, 1,  $\sqrt{2}$ , and 2 (13 possible velocity vectors) [3].

### Self-similar flow

Under certain conditions the flow at the expansion of a rectilinear conductive channel can be self-similar. For the one-dimensional problem of expansion of a conductive channel, a self-similar solution was derived (Fig. 1) which is valid when the following three requirements are satisfied [4].

- The power released in the channel  $W = \text{const}$  (for the cylindrical case  $W = at$  [5]).
- The heat conductivity inside the channel is high, and one can roughly consider that the energy released is completely transferred to the channel boundary by both the conductive heat flux and radiation.

- The total heat flux from the channel is completely absorbed in a thin layer of liquid, leading to transition of the liquid to the plasma of the channel after dissociation and partial ionization of the material. Experimental data on the absorption spectrum of water in the far ultraviolet region indicate that radiation with a wavelength  $\lambda < 1600 \text{ \AA}$  is almost entirely absorbed in a thin layer of liquid  $\sim 10^{-4} \text{ cm}$ .

Under these requirements, the mass velocity of the “plasma” inside the conductive channel is equal to zero, and the temperature, density, and pressure are constant both across the channel section and in time.

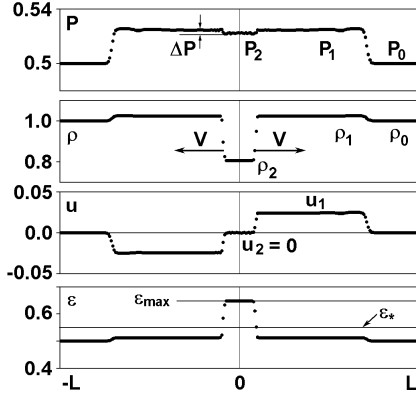


**Fig. 1.** Structure of the self-similar flow obtained by the LBE method for streamer channel expansion. Here  $P$  is the two-dimensional pressure,  $\rho$  is the density,  $u$  is the mass velocity, and  $\epsilon$  is the average kinetic energy of one particle.

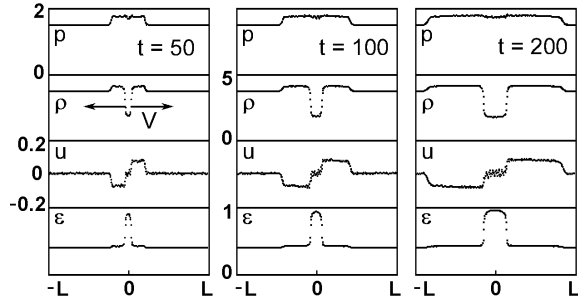


**Fig. 2.** Conductive channel expansion obtained by the LG method. Grid size  $400 \times 20000$ .

Figure 1 shows the structure of the one-dimensional self-similar flow obtained in [4] by the LBE method. Similar results (Fig. 2) were obtained there in a simulation of the channel stage of electric breakdown by the LG method with energy release.

Self-similar regimes of the expansion of a cylindrical streamer channel were investigated for  $W = at$ . Figure 3 shows results obtained by the LBE method. The mass velocity inside the channel was  $u \approx 0$ , and outside it was approximately  $u \sim 1/r$  up to the front of the divergent shock wave. The strength of this wave depended on the energy release and in the present case it was small. As in the LG computations, there were disturbances in the conductive channel, most noticeable on the velocity plots. This was probably connected with the presence of stochastic turbulence in the channel “plasma”.

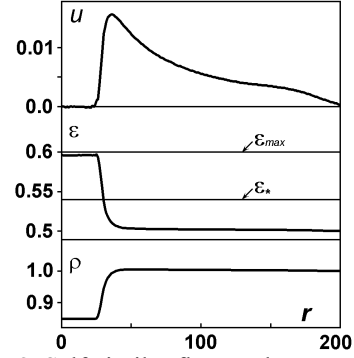


**Fig. 3.** Self-similar flow at the expansion of a cylindrical streamer channel. Time is  $t = 180$ .

### Liquid-“plasma” transition layer

The inner structure of a viscous transition layer of thickness  $L$  is described in a frame of reference moving together with it at velocity  $D$  by the following equations (for low heat conductivity)

$$\rho v = \rho_1 D, \quad p + \rho_1 D v - \left( \frac{4}{3} \eta + \zeta \right) \frac{dv}{dx} = p_1 + \rho_1 D^2,$$

$$\frac{\gamma}{\gamma-1} \rho v + \rho_1 D \frac{v^2}{2} - \left( \frac{4}{3} \eta + \zeta \right) v \frac{dv}{dx} = \frac{\gamma}{\gamma-1} p_1 D$$

$$+ \rho_1 \frac{D^3}{2} + v \int_0^x \frac{Q}{v} dx.$$

Here  $v$  is the current mass velocity,  $\gamma$  is the adiabatic index of gas in a transition layer,  $Q$  is the heat release per unit volume,  $\eta$  is the shear viscosity, and  $\zeta$  is the second viscosity. The pressure  $p_1$  in the liquid near the cylindrical discharge channel can be estimated from its expansion velocity  $V$  [6]. For  $V \sim 100 \text{ m/s}$ , one has for water  $p_1 \approx 3 \cdot 10^7 \text{ Pa}$ .

If the thickness of the transition layer is much less than the channel radius, the transition layer can be treated as a quasi-stationary gas-dynamic discontinuity. There is a small pressure drop at intersection of the transition layer  $\Delta p = \rho_1 D (v_2 - D)$  (inside the channel the pressure is lower). Its magnitude agrees quantitatively with the value obtained in computations by the LBE method (Fig. 1). This effect is caused by the mass inflow through the channel boundary. The addition to the pressure in front of the discontinuity is merely the reactive force due to fast liquid “vaporization”.

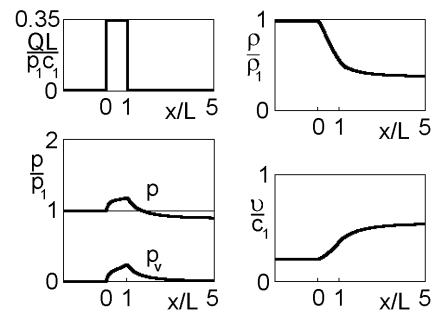


**Fig. 4.** Structure of the viscous transition layer.

The inner structure of the viscous transition layer is shown in Fig. 4. The system of equation was solved for  $p_1 = 1$ ;  $c_1 = 1$ ;  $L = 1$ ;  $D/c_1 = 0.2$ ;  $\gamma = 5/3$ , dimen-

dimensionless viscosity  $(4/3\eta+\zeta) c_1/(p_1L) = 1$ , and dimensionless heat release  $QL/p_1c_1 = 0.35$ . The final mass velocity relative to the zone of energy release can become higher as well as lower than the sound velocity in front of the wave  $c_1$ . There is a pressure peak in the narrow energy release zone ( $p = p_1 + \rho_1 D(D-v) + p_v$ ) because of the viscous part of the stress tensor  $p_v = (4/3\eta+\zeta) dv/dx$ . The magnitude of this peak can be estimated in the case of constant viscosity assuming  $dv/dx \sim V/L$ . For characteristic values  $V \sim 100$  m/s [7],  $\eta = 10^{-3}$  kg/m·s, and  $L \sim 10^{-6}$  m [8], the magnitude of the pressure peak  $\Delta p \sim 10^5$  Pa  $\sim 1\%$  of  $p_1$ .

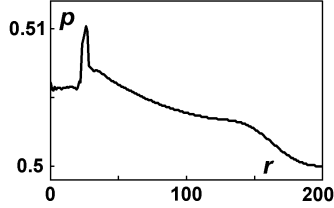


**Fig. 5.** Pressure plot for cylindrical channel expansion. Time is  $t = 160$ .

Figure 5 shows the radial dependence of pressure for the cylindrical self-similar regime (see also Fig. 3). The relative magnitude of the pressure peak in the transition layer is  $\Delta p/p_1 \sim 1\%$ .

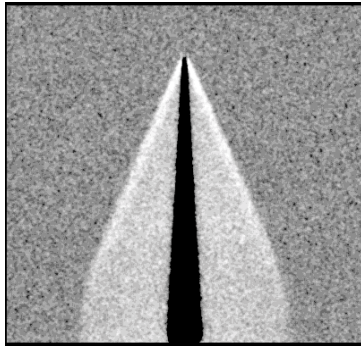


**Fig. 6.** Density distribution.  $v \approx 2.5 C$ ,  $t = 140$ .

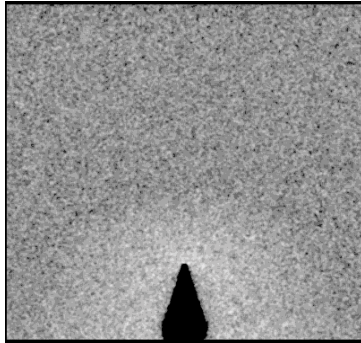


**Fig. 7.** Density distribution.  $v \approx 0.5 C$ ,  $t = 200$ .

#### Propagation of the tip of linear conductive channel

The propagation of the tip of a linear conductive streamer channel was simulated [9]. Figures 6 and 7 show density distributions of the material averaged over 15 realizations in computations by the LG model [10] with eight directions and three values of particle velocity 0, 1, and  $\sqrt{2}$  on a grid  $400 \times 400$ . The dark color corresponds to the lower density (negative image). Conductive channel expansion and a formation

of compression waves were observed. These waves moved at the sound velocity in a dielectric liquid  $C \approx 0.95$ . When the velocity of the streamer tip was greater than  $C$ , a divergent shock wave having a nearly conical front was formed. Such waves have been observed experimentally [7]. In the case of lower velocities of the streamer tip propagation, the wave front became spherical. This compression wave was not always a shock wave.

The density distribution obtained by the LBE method [9] for some values of streamer tip velocity  $v$  are shown in Fig. 8. Here the dark color also corresponds to the lower density.

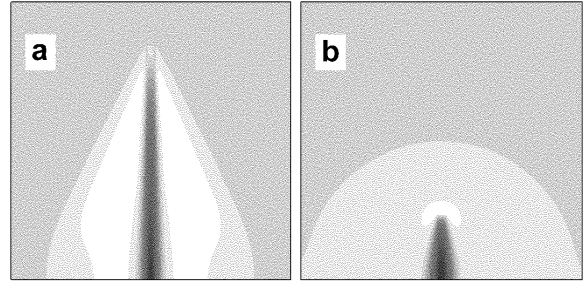


**Fig. 8.** Density distribution.  $a - v = 2.5 C$ ,  $t = 100$ ;  $b - v = 0.5 C$ ,  $t = 140$ .

#### Growth of streamer structures in a viscous dielectric liquid

A model was realized in which two-dimensional flow of a dielectric liquid is simulated by the ILG method [1] and the transition of the dielectric to the conductive phase is described by the field fluctuation criterion (FFC) [11,12]. In this case, the streamer structure grows as a result of both breakdown of new portions of the dielectric and hydrodynamic expansion of the already existing conductive region.

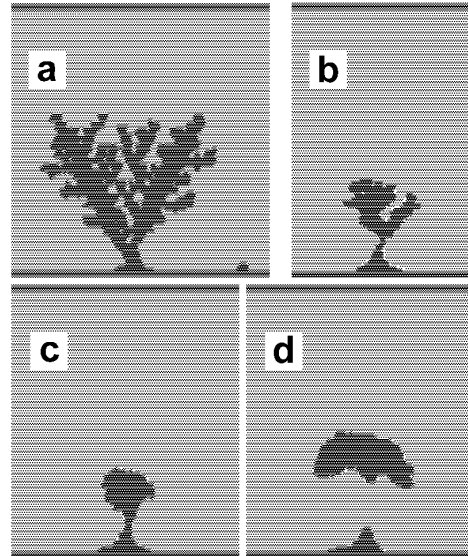


**Fig. 9.** Shape of the conductive region. (a) branched streamer structure (grid  $113 \times 130$ ),  $t = 40$ ; (c) and (d) are bubble-like streamer development (formation of a vortex), (c)  $t = 200$ ; (d)  $t = 350$ ; (b) intermediate case.

Transition between these two mechanisms of the conductive structure development was demonstrated.

Figure 9a gives an example of the formation of a branched streamer structure mainly by breakdown of new portions of the dielectric. The characteristic growth speed was almost twice the sound velocity  $C$  and depended on the electric-field strength in front of the streamer tip. The streamer structure growth mainly due to hydrodynamic flow is shown in Fig. 9c–d. A conductive region of bubble-like shape was accelerated by electrodynamic forces. The characteristic growth speed of such structure was about  $0.2 C$ . In this case, a flow in the form of a vortex dipole moving toward the upper electrode is clearly seen at late stages. This kind of the breakdown process development has been observed in experiments on breakdown of high-viscosity liquids [13] and in certain regimes of partial breakdown [14]. The intermediate case is presented in Fig. 9b.

#### Growth of a branched streamer structure with formation of shock waves

Most of the existing stochastic growth criteria allow the formation of new conductive bonds at any place on the boundary of the conductive structure [15]. The currently available high-speed photographs of the breakdown development show that the streamer growth usually occurs only from the tips of existing branches [16].

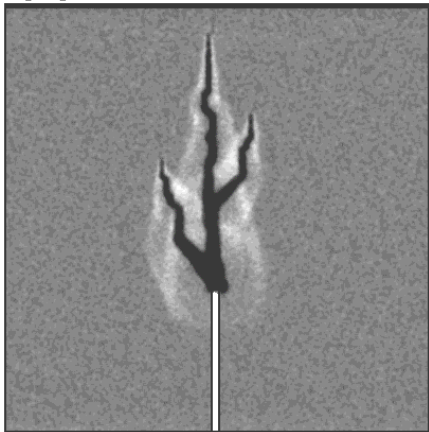


**Fig. 10.** Shape of the streamer structure and the pattern of divergent shock waves (grid  $400 \times 400$ ),  $t = 50$ .

A model was realized in which liquid flow is simulated by the LG method with energy release [4,10] and the growth of the streamer tips is described by the tip growth criterion with ramification (TGCR). At the first computation stage, the growth of the streamer structure was computed using the TGCR model ignoring gas-dynamic flows. The distribution of the electric-field potential was computed at each time step by solving the Poisson equation, and the charge transport along the streamer conductive branches was determined from the Ohm law. At the second stage, computations were carried out of the gas-dynamic flows formed for the fixed sequence of growth of the streamer branches. Distributions of the material density were averaged over 9 neighboring sites of the lattice and some stochastic realizations of gas-dynamic flows. Figure 10 shows an example of the growth of a branched streamer structure from a point electrode.

The average velocity of growth of the branches was 2–5 times higher than the sound velocity. The density distribution averaged over 12 realizations is shown. The dark color corresponds to the lower density (negative image). Shock waves diverging from the streamer tips are clearly seen. When these waves interacted with each other and with the streamer channels, a complex interference flow pattern arose that was usually observed experimentally [7].

Gas-dynamic processes are shown, on the one hand, to be a result of the streamer growth and, on the other hand, to have a crucial effect on the growth dynamics of streamer structures.

This work was supported by the Russian Foundation for Basic Research grant No. 97-02-18416.

#### References

- [1] U. Frisch, B. Hasslacher and Y. Pomeau, *Phys. Rev. Lett.*, Vol. 56, No. 14, pp. 1505-1508, 1986.
- [2] P. Bhatnagar, E. P. Gross and M. K. Krook, *Phys. Rev.* Vol. 94, pp. 511-525, 1954.
- [3] Y. H. Qian, *J. Sci. Comp.* Vol. 8, No. 3, pp. 231-242, 1993.
- [4] A. L. Kupershtokh and D. A. Medvedev, *Conf. Record of the 1998 IEEE Int. Symp. on Electrical Insulation*, Arlington, USA, pp. 611-614, 1998.
- [5] V. V. Arsent'ev, *J. Appl. Mech. Tech. Phys.*, No. 5, pp. 34-37, 1965.
- [6] I. Z. Okun', *Izv. Akad. Nauk SSSR, Mekh. Zhidk. Gaza*, No. 1, pp. 126-130, 1965.
- [7] P. Gournay and O. Lesaint, *J. Phys. D: Appl. Phys.*, Vol. 27, pp. 2117-2127, 1994.
- [8] A. L. Kupershtokh, *Proc. of the 15th Int. Conf. on Phenomena in Ionized Gases*, Minsk, USSR, pp. 345-346, 1981.
- [9] A. L. Kupershtokh and D. A. Medvedev, *Proc. of V Int. Conf. "Contemporary Problems of Electrophysics and Electrohydrodynamics of Liquids"*, St. Petersburg, Russia, pp. 126-130, 1998.
- [10] A. L. Kupershtokh, S. M. Ishchenko, A. P. Ershov, *Proc. of the 12th Int. Conf. on Conduction and Breakdown in Dielectric Liquids*, Roma, Italy, pp. 107-110, 1996.
- [11] A. L. Kupershtokh, *Sov. Tech. Phys. Lett.* Vol. 18, No. 10, pp. 647-649, 1992.
- [12] A. P. Ershov, A. L. Kupershtokh, *Proc. of the 11th Int. Conf. on Conduction and Breakdown in Dielectric Liquids*, Baden-Dättwil, Switzerland, pp. 194-198, 1993.
- [13] P. K. Watson, W. G. Chadband, M. Sadeghzadeh-Araghi, *IEEE Trans. Elec. Insul.*, Vol. 26, No. 4, pp. 543-559, 1991.
- [14] H. Yamashita, K. Yamazawa, W. Machidori and Y. S. Wang, *Proc. of the 12th Int. Conf. on Conduction and Breakdown in Dielectric Liquids*, Roma, Italy, pp. 226-229, 1996.
- [15] D. I. Karpov and A. L. Kupershtokh, *Conf. Rec. of the 1998 IEEE Int. Symp. on Elec. Insul*, Arlington, Virginia, pp. 607-610, 1998.
- [16] Y. Torshin, *Proc. of the 12th Int. Conf. on Conduction and Breakdown in Dielectric Liquids*, Roma, Italy, pp. 230-233, 1996.